

Topical Review

Na⁺ Recirculation and Isosmotic Transport

E.H. Larsen, N. Møbjerg

Department of Molecular Biology, University of Copenhagen, August Krogh Building, Universitetsparken 13, DK-2100 Copenhagen Ø, Denmark

Received: 5 June 2006/Revised: 5 September 2006

Abstract. The Na⁺ recirculation theory for solute-coupled fluid absorption is an expansion of the local osmosis concept introduced by Curran and analyzed by Diamond & Bossert. Based on studies on small intestine the theory assumes that the observed recirculation of Na⁺ serves regulation of the osmolarity of the absorbate. Mathematical modeling reproducing bioelectric and hydrosmotic properties of small intestine and proximal tubule, respectively, predicts a significant range of observations such as isosmotic transport, hyposmotic transport, solvent drag, anomalous solvent drag, the residual hydraulic permeability in proximal tubule of AQP1 (–/–) mice, and the inverse relationship between hydraulic permeability and the concentration difference needed to reverse transepithelial water flow. The model reproduces the volume responses of cells and lateral intercellular space (*lis*) following replacement of luminal NaCl by sucrose as well as the linear dependence of volume absorption on luminal NaCl concentration. Analysis of solvent drag on Na⁺ in tight junctions provides explanation for the surprisingly high metabolic efficiency of Na⁺ reabsorption. The model predicts and explains low metabolic efficiency in diluted external baths. Hyperosmolarity of *lis* is governed by the hydraulic permeability of the apical plasma membrane and tight junction with 6–7 mOsm in small intestine and ≤ 1 mOsm in proximal tubule. Truly isosmotic transport demands a Na⁺ recirculation of 50–70% in small intestine but might be barely measurable in proximal tubule. The model fails to reproduce a certain type of observations: The reduced volume absorption at transepithelial osmotic equilibrium in AQP1 knockout mice, and the stimulated water absorption by gallbladder in diluted external solutions. Thus, it indicates cellular regulation of

apical Na⁺ uptake, which is not included in the mathematical treatment.

Key words: Solute-coupled water transport — Hertz' convection-diffusion equation — Mathematical modeling — Small intestine — Proximal tubule — Paracellular transport — Aquaporin-1 knockout — Solvent drag — Pseudo-solvent drag

Introduction

It is a general feature of bulk water movement between body compartments that the transported fluid is in near osmotic equilibrium with the extracellular fluid. Early studies revealed a decisive dependence on sodium transport by demonstrating proportionality between rate of volume flow and active Na⁺ flux and significant reduction of fluid transport following ouabain treatment (Curran & Solomon, 1957; Windhager et al., 1958; Diamond, 1962; 1964a; 1964b). These observations led to the hypothesis that the water flux is secondary to the active sodium flux by osmotic coupling between ions and water in an intraepithelial compartment (Curran, 1960; Curran & Macintosh, 1962). In a morphological study of gallbladder, Whitlock and Wheeler (1964) suggested that the coupling compartment is the lateral intercellular space of the epithelium. Diamond and Bossert (1967) provided the first comprehensive theoretical study of the geometry and boundary conditions of the lateral space for generating an isosmotic absorbate which resulted in their standing gradient theory. Testing of the concept of a lateral coupling compartment has generated numerous important experimental and theoretical papers (reviewed in: Sackin & Boulpaep, 1975; Weinstein & Stephenson, 1981; Weinstein 1992; Whittembury & Reuss, 1992; Boulpaep et al., 1993; Weinstein, 1994; Spring, 1998; Schultz, 2001), Concepts of the standing

Correspondence to: E.H. Larsen; email: EHLarsen@aki.ku.dk

gradient theory including water-impermeable tight junctions were further explored in a recent theoretical study of isosmotic transport by simple local osmosis (Mathias & Wang, 2005). Quite different ideas have been proposed by Fischbarg and coworkers who have discussed experimental and theoretical evidence for fluid movement in tight junctions of corneal epithelium by way of electro-osmosis (Sanchez et al., 2002; Rubashkin et al., 2005). As an alternative to the standing-gradient theory Ussing suggested the sodium-recirculation theory of isosmotic transport, which was developed in experimental studies on fluid secretion (Ussing & Eskesen, 1989; Ussing et al., 1996) and fluid absorption (Ussing & Nedergaard, 1993; Nedergaard et al., 1999). Its application to absorbing epithelia is the major subject of the present review.

Isosmotic or near-isosmotic transport constitutes just one of several features characterizing solute-coupled water transport. Focusing only on this function inevitably leads to a framework with limited explanatory range considering the experimental observations that have accumulated over the past 50 years:

- i. The transported fluid is in osmotic equilibrium with the surrounding solutions.
- ii. Isosmotic transport takes place with no external driving force for water.
- iii. Water can be transported against an adverse osmotic gradient, i.e., uphill, and there is an inverse relationship between the transepithelial hydraulic permeability and the osmotic concentration difference at which the water flux becomes zero.
- iv. The major transepithelial electrical conductance is paracellular.
- v. The metabolic cost of sodium uptake varies among epithelia and with the experimental protocol. From about 12 to about 30 moles Na^+ absorbed per mole O_2 consumed, which is below and above, respectively, the cost of $\sim 18 \text{ Na}^+/\text{O}_2$ of the Na^+/K^+ -pump.
- vi. Solvent drag is observed, that is, water absorption is associated with convection fluxes of large water-soluble and plasma membrane-impermeable molecules like dextrans, inulin, sucrose, and mannitol.
- vii. Anomalous solvent drag has been described, which refers to an inwardly directed convection flux of hydrophilic solutes paralleled by a net outward flux of water.

The challenge to any theory of isosmotic transport is that it must have capacity to predict and explain the above features in a logical and coherent way. Comparable to three recent papers on solute-coupled water transport (Weinstein, 2003; Fischbarg & Diecke, 2005; Mathias & Wang, 2005) the present review is a

discussion of experimental observations analyzed by mathematical modeling for evaluating successful predictions and shortcomings of the proposed theoretical framework.

THE KEY PROBLEM OF ISOSMOTIC TRANSPORT: CONVECTION-DIFFUSION OF SOLUTES ACROSS THE INTERSPACE BASEMENT MEMBRANE

In Fig. 1 the sodium pump flux is directed into the lateral intercellular space (*lis*) in agreement with the abundant expression of pumps in the lateral membranes of transporting epithelia (Stirling, 1972; Kashgarian et al., 1985; Pihakaski-Maunsbach et al., 2003), which leads to a hyperosmotic and hyperbaric lateral intercellular space. With n osmolytes and similar composition and hydrostatic pressure, respectively, of the solutions bathing the two sides of the epithelium, the water flux, J_V across the barriers delimiting the lateral intercellular space (tight junction, *tj* or interspace basement membrane, *ibm*) is given by the equation (Finkelstein, 1987):

$$J_V = L_P \left[\Delta P - RT \sum_{j=1}^n \sigma_j \Delta C_j \right] \quad (1)$$

L_P is the hydraulic permeability of *tj* or *ibm*, R the universal gas constant, T the absolute temperature, σ_j the reflection coefficients of *tj* or *ibm*, and ΔP and ΔC_j the hydrostatic pressure difference and the concentration differences, respectively, between bath and *lis*. With the reflection coefficients of tight junction being larger than those of the interspace basement membrane, $\sigma_j^{tj} \gg \sigma_j^{ibm} \approx 0$, water is flowing from the outside of the epithelium (lumen) to the blood side. This system has the capacity to drive water also against an adverse transepithelial osmotic gradient, provided the osmotic concentration of *lis* is maintained above the osmotic concentration of the luminal bath. It should be noted that at transepithelial osmotic equilibrium the water flux is directed into the cells from *both* sides of the epithelium. It follows that all of the water flowing into the epithelium will leave the epithelium through the interspace basement membrane.

If the water permeability of the apical barriers is large a steady state would be achieved with near-osmotic equilibrium between *lis* and the external baths. However, one cannot assume that the fluid leaving *lis* would also be in near-osmotic equilibrium with the external solutions. The solute concentration of the fluid leaving *lis* through the interspace basement membrane is governed by Hertz' convection-diffusion equation (Hertz, 1922). Applied to a homogenous membrane with reflection coefficient, σ_s , and considering an uncharged solute for convenience, the equation takes the form:

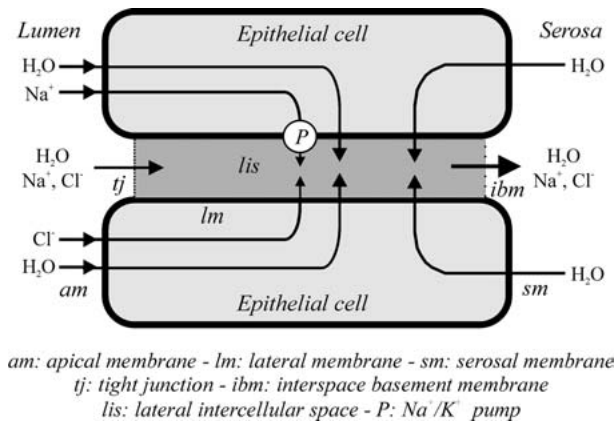


Fig. 1. The ‘local osmosis’ model of solute-coupled fluid absorption driven by lateral Na⁺/K⁺ pumps. K⁺ fluxes are not included and Na⁺ and Cl⁻ fluxes are shown in different cells for convenience. With solutions of identical composition on the mucosal and serosal side, water is entering the cells both through the apical and the serosal (basal) plasma membrane. Water then leaves the epithelium entirely through the interspace basement membrane.

$$\frac{J_S}{J_V} = (1 - \sigma_S) \frac{C_S^{\text{dis}} - C_S^{\text{serosa}} \cdot \exp[-(1 - \sigma_S)J_V/P_S]}{1 - \exp[-(1 - \sigma_S)J_V/P_S]} \quad (2)$$

J_S and J_V are the solute and volume flux across the interspace basement membrane (*ibm* of Fig. 1), respectively, C_S^{dis} and C_S^{serosa} are the solute concentrations on the two sides of the boundary, while P_S is its solute permeability. It follows that the fluid emerging from the basal exit of *lis* would have a composition identical to that of *lis* if one makes the volume flux J_V tend to infinity. It turns out, however, that for systems discussed here the ratio, J_V/P_S , is not very large. Hence the flux of a solute leaving *lis* contains a significant diffusion component together with the convection component resulting in an emerging fluid that is hyperosmotic (calculated as J_S/J_V) relative to the fluid in *lis* (and baths).

For illustrating the problem, Fig. 2 depicts the concentration of the emerging fluid as a function of the volume flux out of *lis* at three different solute permeabilities of *ibm* that cover likely values of vertebrate epithelia. The reflection coefficient, which supposedly is small, is set to $\sigma_S = 10^{-3}$. The equivalent resistances of *ibm* are also given in Fig. 2 for indicating the physiological relevance of chosen solute permeabilities. They have been calculated by the equation (Sten-Knudsen, 2002):

$$R^{\text{ibm}} = \frac{R \cdot T \cdot (C_S^{\text{lis}} - C_S^{\text{serosa}})}{F^2 \cdot C_S^{\text{lis}} \cdot C_S^{\text{serosa}} \cdot P_S^{\text{ibm}} \cdot \ln(C_S^{\text{lis}}/C_S^{\text{serosa}})} \quad (3)$$

Eq. 3 is valid for monovalent ions near equilibrium with $R = 8.31 \text{ Joule} \cdot \text{K}^{-1} \cdot \text{mol}^{-1}$, $T = 310^\circ \text{ K}$, and $F = 96485 \text{ Coul} \cdot \text{mol}^{-1}$. The calculations shown in numbers in Fig. 2 represent the volume flux of rat

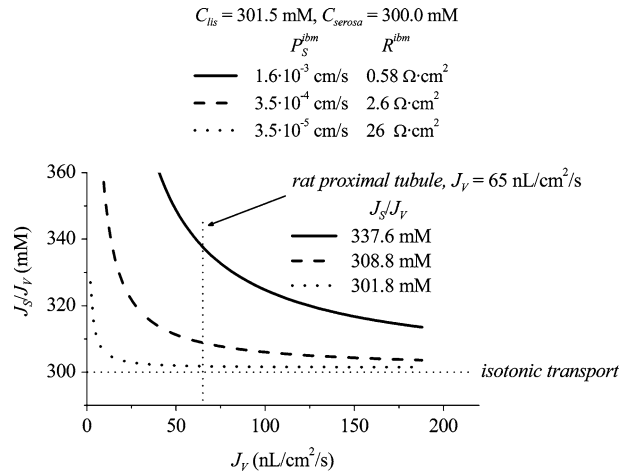


Fig. 2. The concentration of the fluid emerging from the lateral intercellular space is governed by Hertz’ equation (text Eq. 2). The graphs indicate the concentration of the emerging fluid as function of the volume flow through the interspace basement membrane (*conf.* Fig. 1). Increasing solute permeability and decreasing water flow raises the concentration of the emerging fluid, which rises far above the concentration of the lateral space.

proximal tubule ($65 \text{ nL} \cdot \text{cm}^{-2} \cdot \text{s}^{-1}$). Due to its very high water permeability it is not unlikely that the osmotic concentration of *lis* is quite close to that of the bathing solutions (*see below*). In the calculations shown here it is assumed that $C_S^{\text{lis}} = 301.5 \text{ mOsm}$ for $C_S^{\text{serosa}} = 300 \text{ mOsm}$, that is, the difference of 0.5% is so small that it would be impossible to detect it by available methods. It can be seen that even with the chosen very small hyperosmolarity of *lis* and with a permeability of *ibm*, which is in the range of estimated values for rat proximal tubule, corresponding to $R^{\text{ibm}} = 0.6 \Omega \cdot \text{cm}^2$ (Weinstein, 1992), the emerging fluid would be significantly hyperosmotic (337.6 mOsm versus 301.5 and 300 mOsm, respectively). With a similar flow rate and for $R^{\text{ibm}} = 2.6 \Omega \cdot \text{cm}^2$ the absorbate is near-isosmotic. At an even smaller solute permeability, corresponding to $R^{\text{ibm}} = 26 \Omega \cdot \text{cm}^2$, J_S/J_V is practically equal to C_S^{lis} . However, with a paracellular resistance of 5–10 $\Omega \cdot \text{cm}^2$ in proximal tubule, values of $R^{\text{ibm}} > 2 \Omega \cdot \text{cm}^2$ may be too high. The conclusion is that because the convection is overlaid by diffusion it is by no means justified assuming similar solute concentration of *lis* and the fluid flowing out of *lis*.

Isosmotic Transport

In the standing-gradient theory of Diamond and Bossert (1967) the diffusion flux from the lateral intercellular space is eliminated by assuming the boundary condition, $(dC_S/dx)^{\text{ibm}} = 0$. Thus, with $\sigma_S = 0$ we obtain $J_S/J_V = C_S^{\text{serosa}}$ (*conf.* Eq. 2), corresponding to truly isosmotic transport. The

Na^+/K^+ -pumps were assumed concentrated at the upper end of the closed lateral intercellular space for creating a local hyperosmotic fluid in *lis*. The osmotic gradient is subsequently dissipated as the fluid moves toward the open end of *lis* and more water is added by osmosis from cells.

A quite different solution to the problem of isosmotic transport assumes that ions are being recirculated back into *lis* by a regulated Na^+ -gradient-driven ion transporter in the basal plasma membrane (Ussing & Nedergaard, 1993; Nedergaard et al., 1999). According to this concept the generation of an isosmotic absorbate is regulated and depending on ATP consumption by the lateral Na^+/K^+ -pumps both for creating a hyperosmotic fluid in *lis* and for adjusting the transported fluid to the demanded osmolarity. This theory does not require non-uniform distribution of pumps and channels on the lateral intercellular membranes, and even in its most simple design with well-stirred lateral space it appears to work well with relevant combinations of physiological observables (Larsen et al., 2000; 2002). It is the intention of the present review to focus on the concept of ion recirculation and its quantitative applications to the relatively water-tight small intestine and the highly water-permeable proximal tubule.

Small Intestine

Small intestine is a 'leaky' epithelium with a low-resistance paracellular shunt and rheogenic active Na^+ transport (Barry et al., 1965; Frizzell & Schultz, 1972; Halm et al., 1985a). Large amounts of fluid are crossing the intestinal wall, in human subjects as much as 5–6 liters per day. In response to manipulating the transepithelial gradients of osmotic concentration in absence of solute uptake, water is moving freely across the intestinal epithelium and into lumen if the mucosal bath is made sufficiently hyperosmotic with respect to the serosal bath. Fluid uptake can take place against a considerable adverse osmotic gradient, e.g., 145 mosm·kg⁻¹ in rat jejunum (Parsons & Wingate, 1958) and 75 mosm·kg⁻¹ in rabbit ileum (Naftalin & Tripathi, 1986). Under physiological conditions, however, salt and water are transported in the inward direction in such a way that the absorbate is isosmotic with the mucosal fluid (Curran & Solomon, 1957). Furthermore, fluid is flowing in the inward direction in the absence of an osmotic gradient, but if the net solute uptake is stopped the net water movement also stops (Curran, 1960). Curran concluded that by depending on the active uptake of salt the fluid uptake as well depends on energy metabolism of the intestinal epithelial cells.

STRATEGY OF EXPERIMENTAL APPROACH

Since water flow is secondary to fluxes of sodium it is important to identify the pathways taken by this ion and the fluxes through these pathways. Unidirectional sodium fluxes through toad small intestine were studied by the method of pre-steady state flux-ratio analysis, which can be applied for any combination of transport mechanisms (electrodifusion, convection, active transport, co-transport, etc.) provided the epithelium is in a physiological steady state. With this method advantage is taken of the theoretical result that for a single pathway the ratio of unidirectional fluxes is time-invariant and equal to the value of the stationary flux ratio (Steen-Knudsen & Ussing, 1981). Thus, if the flux ratio is time-variant, more than one pathway is available for transport of the ion. While the flux ratio of ¹³⁷Cs⁺ turned out to be time-invariant with the steady state being reached relatively fast as compared to ⁴²K⁺ fluxes, the ratio of ²⁴Na⁺ could be split up into two components of different time constants (Nedergaard et al., 1999). These results were interpreted in the following way: Only the paracellular pathway is available for transepithelial fluxes of ¹³⁷Cs⁺, whereas ²⁴Na⁺ is transported along the paracellular as well as the cellular pathway. This interpretation agrees with the finding that ¹³⁷Cs⁺ entering epithelial cells via the Na^+/K^+ -pump are being trapped in the cellular compartment (Nedergaard et al., 1999). Thus, transepithelial tracer fluxes of Cs⁺ must have taken a paracellular pathway. The results compiled in Table 1 were used for estimating the mechanism of paracellular transport as well as the recirculation flux of Na⁺.

PARACELLULAR FLUX-RATIO ANALYSIS: EVIDENCE FOR PARACELLULAR WATER UPTAKE

With identical concentrations on the two sides of the epithelium and with a transepithelial electrical potential difference of $V_T = -3.9$ mV (Table 1) simple electrodiffusion of a monovalent cation would result in the following flux ratio (Ussing, 1949):

$$\frac{J_{\text{Na}}^{\text{para, in}}}{J_{\text{Na}}^{\text{para, out}}} = \frac{J_{\text{Cs}}^{\text{para, in}}}{J_{\text{Cs}}^{\text{para, out}}} = \frac{C_j^{\text{lumen}}}{C_j^{\text{serosa}}} \exp \frac{zFV_T}{RT} = 0.86 \quad (4)$$

Not only are the measured flux-ratios above—not below—unity, but they are also different from one another (Table 1). This would indicate a different inwardly directed driving force acting on the two ions, which exceeds the outward force associated with the lumen-negative V_T . Solvent drag, which discriminates between the ions according to their atomic diameter, would be a most likely candidate. Formally it is possible to set up a flux-ratio equation that takes into account interactions of ions and water in the delimiting membranes of *lis* (Larsen et al., 2002):

Table 1. Experimental and computed transepithelial potential difference (V_T) and ion fluxes in small intestine

	V_T mV	J_{Na}^{Net}	$J_{Na}^{Para, in}$ pmol/s/cm ²	$J_{Na}^{Para, out}$	$J_{Na}^{Para, in} / J_{Na}^{Para, out}$	$J_{Cs}^{Para, in} / J_{Cs}^{Para, out}$	Na ⁺ Recirculation
Expt.*	-3.9 ± 1.8	773 ± 56	450 ± 40	130 ± 20	3.66 ± 0.34	2.06 ± 0.12	0.65 ± 0.03
Model [#]	-3.7	1083	395.2	108.4	3.65	2.21	0.63

*From Nedergaard et al. 1999. [#] From Larsen et al. 2002. Na⁺ recirculation is here indicated at percentage of sodium ions pumped into the lateral space that is derived from serosal bath. It is calculated by Eq. 8.

$$\frac{J_j^{para, in}}{J_j^{para, out}} = \frac{C_j^{lumen}}{C_j^{serosa}} \exp \frac{zFV_T}{RT} \cdot \exp \left[\frac{(1 - \sigma_j^{ij}) J_V^{ij}}{P_j^{ij}} + \frac{(1 - \sigma_j^{ibm}) J_V^{ibm}}{P_j^{ibm}} \right] \quad (5)$$

Here, J_V and P_j denote the water flux and the ion permeability, respectively, of the membrane barrier indicated by superscript. If $J_V^{ij} \approx J_V^{ibm}$, $\sigma_{Na}^{ij} \approx \sigma_{Cs}^{ij}$, $\sigma_{Na}^{ibm} = \sigma_{Cs}^{ibm} \approx 0$ and $P_{Na}^{ij} \ll P_{Na}^{ibm}$, $P_{Cs}^{ij} \ll P_{Cs}^{ibm}$, and with two monovalent cations sharing paracellular translocation route, Eq. 5 reduces to an expression of the type:

$$\frac{J_{Cs}^{para, in}}{J_{Cs}^{para, out}} = \left(\frac{J_{Na}^{para, in}}{J_{Na}^{para, out}} \right)^{\frac{P_{Na}^{ij}}{P_{Cs}^{ij}}} \quad (6)$$

If it is assumed that the tight junction discriminates between the two ions according to their diffusion coefficients in water, i.e., $P_{Na}^{ij} / P_{Cs}^{ij} \approx D_{Na} / D_{Cs} = 0.66$, one predicts (Eq. 6 and Table 1) a ratio of paracellular Cs⁺ fluxes of 2.2. This in fact is not significantly different from the measured ratio of 2.06 ± 0.12 (Table 1), indicating that solvent drag on the two ions causes the deviation of their flux ratios from the ratio of electrodiffusion fluxes (Eq. 4). Thus, from being peculiar deviations from Eq. 4, the two experimental flux ratios follow logically from the assumption of transjunctional water flow between the epithelial cells. This interpretation is in accordance with earlier studies on streaming potentials across small intestine, indicating convection fluxes of small ions through lateral spaces (Smyth & Wright, 1966).

INTERPRETATION OF UNIDIRECTIONAL CELLULAR Na⁺ FLUXES: CALCULATION OF THE RECIRCULATION FLUX

The two unidirectional cellular fluxes listed in Table 1 are associated with the lateral sodium pump as shown in Fig. 3. According to this interpretation, the lateral pumps constitute a source delivering the radioisotope into the reversible paracellular pathway, which will not affect the ratio of transepithelial unidirectional fluxes:

$$\frac{J_{ms}^{cell}}{J_{ms}^{cell, return}} = \frac{J_{Na}^{para, in}}{J_{Na}^{para, out}} \quad (7a)$$

$$\frac{J_{sm}^{cell, return}}{J_{sm}^{cell}} = \frac{J_{Na}^{para, in}}{J_{Na}^{para, out}} \quad (7b)$$

With the above set of equations and the fluxes estimated by experiments (J_{ms}^{cell} and J_{sm}^{cell} , Table 1) the two return fluxes were calculated (Table 2). An estimate of the recirculation flux can then be obtained according to:

$$\frac{J_{Na}^{serosa \rightarrow cell \rightarrow lis}}{J_{Na}^{pump}} = \frac{J_{sm}^{cell} + J_{sm}^{cell, return}}{J_{ms}^{cell} + J_{ms}^{cell, return} + J_{sm}^{cell} + J_{sm}^{cell, return}} \quad (8)$$

In experiments with the intestinal preparations a recirculation flux of 0.65 ± 0.03 was obtained. In other words, the above calculations indicated that 65% of the sodium ions pumped into the lateral intercellular space is derived from the serosal bath, while the minor component of 35% enters from the luminal solution via the apical membrane before it is pumped into *lis*.

MATHEMATICAL MODELING OF TRANSPORT BY SMALL INTESTINE

The large recirculation flux estimated above was of considerable concern as it indicated an implausibly high NaCl concentration of the lateral intercellular fluid. For analyzing the problem in details it was decided to develop a mathematical model of the epithelium, in the first place with electroneutral solutes, an approach that was subsequently extended by incorporating charged diffusible elements (Na⁺, K⁺, Cl⁻) and glucose together with a non-diffusible intracellular anion (A^{-n}). With a single cell type and a lateral extracellular space the model contains 5 membrane barriers. The forces driving solute and water fluxes across the individual membranes are due to gradients of electrical potentials, ion and osmotic concentrations, and hydrostatic pressures. They all

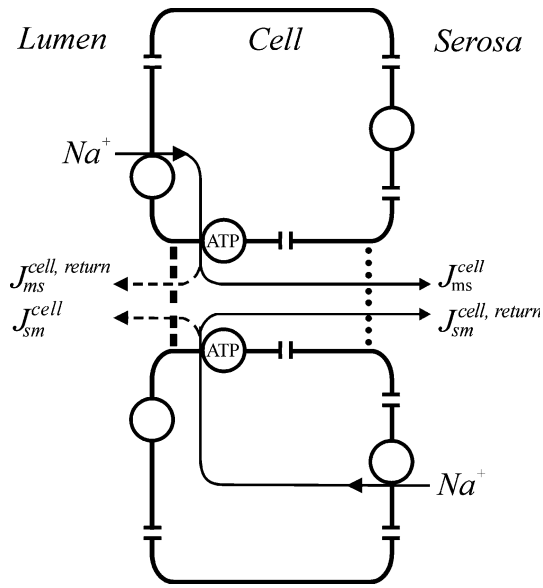


Fig. 3. Interpretation of unidirectional cellular fluxes in small intestine with *ms* and *sm* indicating the ‘mucosa to serosa’ and ‘serosa to mucosa’ direction, respectively. With the Na^+/K^+ -ATPase on the lateral plasma membrane, Na^+ fluxes in both directions enter the lateral space via sodium pumps. Whether the flux departs from the luminal or the serosal solution, a fraction of the pumped flux returns to the departing compartment with the associated fluxes indicated by $J_{ms}^{\text{cell, return}}$ and $J_{sm}^{\text{cell, return}}$, respectively. $J_{ms}^{\text{cell, return}}$ is expected to be relatively large because water is flowing in the inward direction. The directly measured unidirectional fluxes are J_{ms}^{cell} and J_{sm}^{cell} , respectively, while the two return fluxes can be estimated by Eqs. 7a and b.

Table 2. Sodium fluxes defined in Fig. 3 and calculated according to Eqs. 7a and b ($N = 5$ preparations). From Nedergaard et al. 1999.

J_{ms}^{cell}	$J_{ms}^{\text{cell, return}}$ $\text{pmol}\cdot\text{cm}^{-2}\text{ s}^{-1}$	J_{sm}^{cell}	$J_{sm}^{\text{cell, return}}$
880 ± 130	260 ± 60	430 ± 90	1730 ± 320

have to be included in the mathematical description for obtaining insights about relationships between biophysics of the membranes and their bioelectrical features, interactions between water and ion fluxes, and conditions for solute-coupled fluid transport. The outline of the model is given in Fig. 4. The model contains equations for ion and water fluxes based upon electrodiffusion and convection theory, and empirical equations handling transport by pumps and cotransporters. The steady-state criteria are expressed by mass conservation of all diffusible elements and water, electroneutrality in intraepithelial compartments with the further requirement that the net charge flux across the epithelium is equal to the clamping current (which is zero in the computations shown below). A compliance model of cells and *lis* associated with infinitely large external baths provide

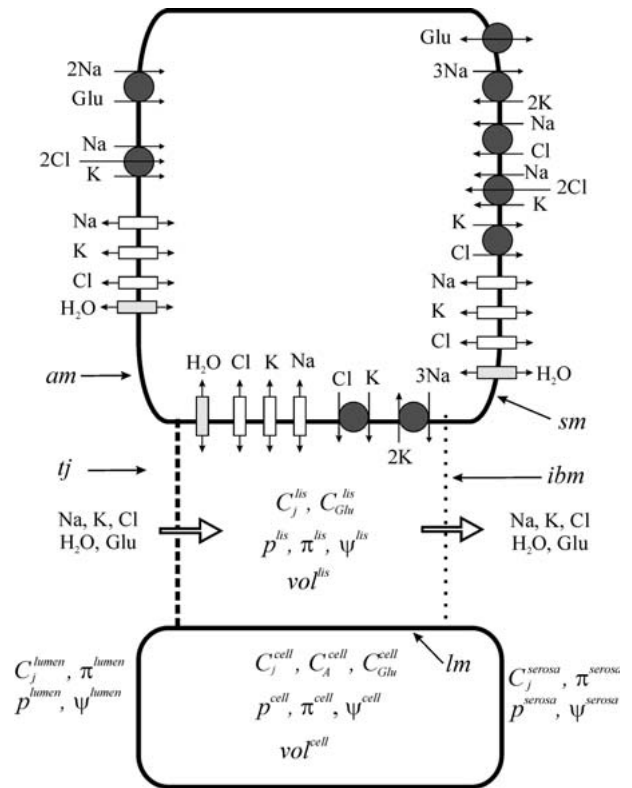


Fig. 4. Transport mechanisms on the three membrane domains of the model epithelium represented by the apical plasma membrane (*am*), the lateral plasma membrane (*lm*), and the serosal (basal) plasma membrane (*sm*). The functional polarity of the model epithelium is given by the transport systems being turned on during computations. The mathematical equations governing the fluxes of ions and water through individual pathways are listed in the original papers (Larsen et al., 2002, 2006). The fourteen dependent variables are the solute concentrations, electrical potentials (serosal bath grounded), and hydrostatic pressures of cells and lateral space together with the transepithelial potential difference (current-clamp mode) or transepithelial current (voltage-clamp mode). With regulated Na^+ recirculation turned on, the kinetic parameter of the Na^+ gradient-driven co-transporter in *sm* becomes a dependent variable, as well, with the extra equation expressing the dependence of the demanded osmolarity on solute and water fluxes through *ibm* and *sm*. Modified from Larsen et al. (2006).

the hydrostatic pressures of the two intraepithelial compartments on which their volumes depend. The independent variables of the model (ion permeabilities, reflection coefficients, kinetic parameters of pumps and cotransporters, hydraulic permeabilities, etc.) were chosen to obtain a good description of all experimental observables like transepithelial ion fluxes, transepithelial electrical potential difference, membrane conductances, intracellular ion concentrations, and membrane potentials. The computed results to be discussed below are robust, that is, perturbations of the independent input variables about their chosen reference values provided mathematical solutions revealing essentially the same features of the model epithelium.

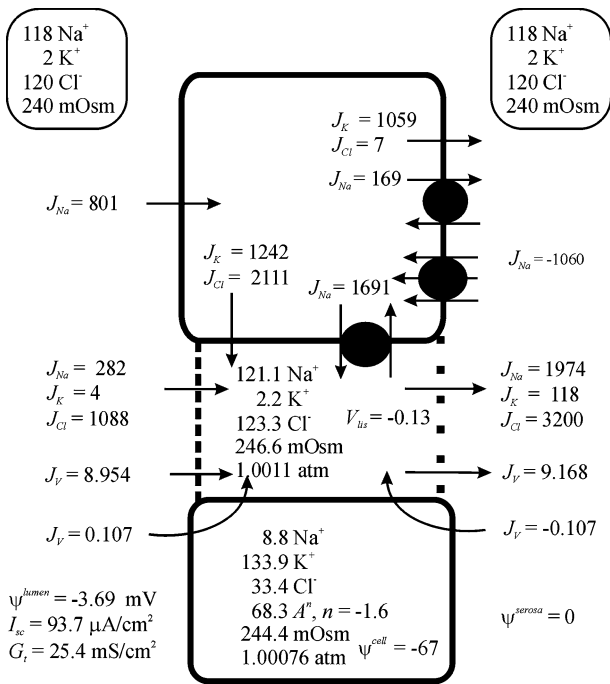


Fig. 5. Reference state of toad small intestine model. $C_{\text{Na}^+}^{\text{lumen}} = C_{\text{Na}^+}^{\text{serosa}} = 118 \text{ mM}$, $C_{\text{K}^+}^{\text{lumen}} = C_{\text{K}^+}^{\text{serosa}} = 2 \text{ mM}$, and $C_{\text{Cl}^-}^{\text{lumen}} = C_{\text{Cl}^-}^{\text{serosa}} = 120 \text{ mM}$. Computed ion concentrations are in mM, electrical potentials in mV, ion fluxes in $\text{pmol}\cdot\text{cm}^{-2}\cdot\text{s}^{-1}$, and volume flow is in $\text{nl}\cdot\text{cm}^{-2}\cdot\text{s}^{-1}$. Regulated Na^+ recirculation is turned on, resulting in truly isotonic transport (240 mOsm) and a recirculation of $-J_{\text{Na}}^{\text{NCCK,sm}}/J_{\text{Na}}^{\text{pump,lm}} = 1060/1691 = 0.63$. This means that 63% of sodium ions pumped into *lis* is derived from the serosal bath in order to achieve truly isotonic transport. Note that despite $C_{\text{Na}^+}^{\text{lis}}$ being not much above $C_{\text{Na}^+}^{\text{bath}}$ (121.1 and 118 mM, respectively), the Na^+ concentration of the fluid emerging from *lis* is, $J_{\text{Na}}^{\text{ibm}}/J_v^{\text{ibm}} = 1974/9.168 = 215 \text{ mM}$, illustrating that the diffusion flux across *ibm* is large relative to the convection flux across this boundary. Modified from Larsen et al. (2002).

COMPUTED RECIRCULATION FLUX

Table 1 compares experimental and computed fluxes and transepithelial potentials and in Fig. 5 is shown the reference intestinal model with computed intracellular concentrations and fluxes of water and ions. The major conclusion is that with the cellular concentrations, membrane potentials, and the transepithelial fluxes correctly simulated, the model computes a recirculation flux of 0.63 when truly isotonic transport is being demanded. This is obtained with a fairly small osmotic concentration difference between *lis* and the serosal bath ($\Delta\pi = 6.6 \text{ mOsm}$, Fig. 5). Nevertheless, with a Na^+ concentration difference of 3.1 mM across the interspace basement membrane the net flux of this ion from *lis* to serosal bath is computed to be $1974 \text{ pmol}\cdot\text{cm}^{-2}\cdot\text{s}^{-1}$. Accordingly, with the water flux of $9.168 \text{ nl}\cdot\text{cm}^{-2}\cdot\text{s}^{-1}$ the Na^+ concentration of the fluid emerging from *lis* is 215 mM. In conclusion, the relatively large recirculation flux estimated from the experiments with the small

intestine does not seem to reflect a particularly high concentration of ions in the lateral space but is associated with fairly large convection-diffusion fluxes across *ibm*. As might be expected this result is not very sensitive to choice of entrance mechanism for Na^+ in the apical brush border membrane. Thus, if an SGLT1 $2\text{Na}^+/\text{glucose}/210 \text{ H}_2\text{O}$ ‘water pump’ is assumed (Loo et al., 1996; Meinild et al., 2001; Zeuthen et al., 2006) computations predicted a Na^+ recirculation flux of 0.56. The somewhat lower recirculation is due to the active component of water uptake generated by the apical cotransporter (Larsen et al., 2002). Furthermore, these computations reproduced the significant contribution of glucose to the total osmotic concentration of the absorbate as discovered by Curran & Solomon (1957). Likewise, a relatively large recirculation flux is predicted with an NKCC transporter being the apical entrance mechanism, as found for the small intestine of the winter flounder (Halm et al., 1985b; see also the original paper by Larsen et al., 2002 for more details).

VALIDATING FURTHER ASPECTS OF THE MODEL

Volume perturbations of intraepithelial compartments result from the integrated response of fluxes across all 5 membranes. Simulations of such changes would underscore the predictive power of the model. The uptake of water and sodium ions, respectively, follow different pathways; water flows through the paracellular pathway, while the Na^+ flux is predominantly translateral. Computations showed that the cell volume as well as the lateral intercellular space volume decreases, by 10% (cell) and 85% (*lis*), respectively, in response to replacing NaCl on the luminal side by a nonpermeant non-electrolyte (Larsen et al., 2002). These predicted volume changes should be compared to observed changes of cell and lateral space volumes of gallbladder exposed on the lumen side to sucrose, which amounted to 23% (cell) and 84% (*lis*), respectively (Spring & Hope, 1979). The large volume change of the lateral space is caused by the decreased pump flux of Na^+ into *lis* whereby the NaCl pool and the water volume of *lis* decreases together with a decrease of the hydrostatic pressure. Elimination of the apical Na^+ uptake per se results in a decrease of the intracellular NaCl pool. However, the associated decrease of $C_{\text{Na}^+}^{\text{cell}}$ leads to an increase of the influx of all three ions via the basal NKCC transporter as well, which would result in an increase of the cellular ion pools. The cell volume change from one steady state to the other depends on these two counter-acting processes.

Kidney Proximal Tubule

Model analysis revealed a fairly strong dependence of the osmotic concentration of *lis* on the hydraulic

permeability of the apical barriers, and predicted decreasing Na^+ recirculation for obtaining an isotonic transportate with increasing hydraulic permeability (Larsen et al., 2000; 2002). This result spurred a recent analysis of ion and water reabsorption by the highly water-permeable kidney proximal tubule to investigate the demand on Na^+ recirculation in computations that faithfully reproduce measured fluxes and bioelectrical characteristics as well as the very high water permeabilities of the plasma membranes. Another purpose was to explore conditions for reproducing the high metabolic efficiency of Na^+ reabsorption and to develop a quantitative description integrating this property with experimental fluxes and electrophysiological characteristics (Larsen et al., 2006).

EXPERIMENTAL STUDIES

A major fraction of the glomerular ultrafiltrate is reabsorbed in the proximal tubules as an isosmotic fluid. Early studies suggested that reabsorption takes place in the absence of external osmotic driving forces driven by active Na^+ transport (Windhager et al., 1958), in agreement with subsequent demonstration of abundant expression of the Na^+/K^+ -ATPase in kidney (Jørgensen, 1981). Nevertheless, it is still a matter of discussion whether water uptake is driven by transepithelial osmotic gradients as well (e.g., Weinstein, 1986; Tripathi & Boulpaep, 1989; Boulpaep et al., 1993; Schafer, 1990; Whitttembury & Reuss, 1992; Weinstein, 1992; Spring, 1998). Luminal dilution towards the distal end of perfused proximal tubules (≤ 3.9 mOsm, depending on absorption rate) has been observed in connection with volume absorption in bilaterally perfused segments with 154 mM-NaCl solutions aerated with 100% O_2 (Green & Giebisch, 1984). The developed luminal hypo-osmolality was eliminated and fluid absorption stopped in cyanide-poisoned preparations, indicating its dependence on metabolic energy (active ion transport). Accordingly, it was speculated that active transport of the solute initially generates a transepithelial osmotic gradient, which more distally drives water through the epithelium of very high hydraulic permeability. A similar mechanism was proposed for fluid reabsorption along the proximal tubule of the AQP1 knockout mouse (Vallon et al., 2000). When 25 mM- NaHCO_3 replaced a similar amount of NaCl in the bath (which then was gassed with 95% O_2 /5% CO_2 , Green & Giebisch, 1984), net volume flow increased, but reabsorption now occurred in the absence of measurable osmotic gradients (< 1.1 mosm $\cdot\text{kg}^{-1}$). It was discussed that fluid uptake under these conditions would be driven by an effective osmotic gradient if the reflection coefficient of NaHCO_3 is greater than that of NaCl. Another way of approaching the problem of solute-coupled water

transport was suggested in a study of bilaterally perfused rat proximal tubule by Green et al., 1991, who demonstrated fluid absorption which could not be accounted for by the prevailing ion gradients nor by the transepithelial hydrostatic and osmotic forces. The active Na^+ flux and the associated solute-coupled water flux were studied in low-bicarbonate perfusates, and were both stimulated by the peritubular protein concentration. The luminal osmotic pressure needed for stopping fluid reabsorption was 11 and 20 mosm $\cdot\text{kg}^{-1}$ H_2O , respectively, in experiments with the two mentioned peritubular protein concentrations. The authors concluded: "This finding places the rat proximal tubule in league with other epithelia, such as small intestine and gallbladder, which transport water both isotonicly and against an adverse osmotic gradient".

Whereas it is widely recognized that bulk water movement across the tubular epithelium is a passive consequence of the active Na^+ transport, it has been much debated whether water is transported entirely across the tubular cells or whether tight junctions constitute additional passage ways for transtubular water uptake (reviewed in, e.g., Berry, 1983; Tripathi & Boulpaep, 1989). However, solvent drag on diffusible ions (Frömter et al., 1973; Schafer et al., 1975) and membrane-impermeable non-electrolytes (Whitttembury et al., 1985; 1988) as well as comparisons of experimental estimates of transtubular and transcellular hydraulic permeabilities (Whitttembury et al., 1985; 1993) point to a significant transjunctional water flow that parallels water uptake along translateral and transcellular pathways. The significant cellular hydraulic permeability is associated with the cloned water channel protein, aquaporin-1 (Denker et al., 1988; Preston et al., 1992), which is expressed at high levels in the apical and basolateral plasma membranes of the proximal tubule (Agre & Nielsen, 1996; Nielsen et al., 2002).

MODELING KIDNEY PROXIMAL TUBULE: SIMPLIFICATIONS AND CHOICE OF VARIABLES

The kinetic constants of the plasma membrane transporters were adjusted to achieve simulation of intracellular ion concentrations and the overall transepithelial fluxes in reasonable agreement with measured values. A major simplification follows from having only three diffusible ions, Na^+ , K^+ , and Cl^- , in the model. Therefore, the bicarbonate and carbonate fluxes associated with specific transporters of the basolateral membrane (Guggino et al., 1983) and the apical $\text{Cl}^-/\text{HCO}_2^-$ and Na^+/H^+ exchange fluxes (Karniski & Aronson, 1985) cannot be reproduced. Another major simplification concerns the ion entrance mechanisms of the apical membrane of which only an NKCC transporter (e.g., Whitttembury et al., 1993) and a Na^+ channel (Gögelein & Greger, 1986)

Table 3. Measured and computed bioelectric properties of proximal tubule with the model's independent variables of solute transporters listed in Larsen et al. 2006 and hydraulic permeabilities listed in Table 4.

	J_V nl·cm ⁻² ·s ⁻¹	J_{Na} nmol·cm ⁻² ·s ⁻¹	V_T mV	R_T Ω·cm ²	$C_{Na^+}^{cell}$ mM	$C_{K^+}^{cell}$ mM	$C_{Cl^-}^{cell}$ mM	V^{cell} mV	R^{apical} Ω·cm ²	f_{Ro}
Rat	65 ^a	9.4 ^a	-2-2 ^{b,c}	5 ^b	17.5 ^d	113 ^e	18 ^f	76 ^b	260 ^b	0.74 ^b
Model	62.1	9.3	-2.9	7.8	15.2	115	12.9	-84	222	0.88

^aWindhager 1979; ^bFrömter 1979; ^cRector 1983; ^dYoshitomi & Frömter 1985; ^eEdelman et al. 1978; ^fCassola et al. 1983.

carry significant fluxes in the computations presented here. It is not a problem per se to omit glucose from the bathing solutions since the NaCl-dependent volume reabsorption takes place in isosmotic proportions also in absence of glucose in the bathing solutions (Windhager et al., 1958; Morel & Murayama, 1970). The advantage of the NKCC transporter is that it allows the simulation of two important transport features of the tubular epithelium, *viz.*, the cellular accumulation of Cl⁻ above equilibrium via an electroneutral apical mechanism and a K⁺ concentration of the absorbate of about 5 mM, which we could not obtain if this ion is transported across the epithelium entirely by paracellular convection. The reflection coefficients of tight junctions were taken from the experimental study of Frömter et al., 1973, and the ion permeabilities and the hydraulic conductance of the paracellular pathway were chosen such as to obtain a paracellular conductance of 5–10 Ω·cm² (Frömter, 1979) and convective flows of the three ions. All independent variables are listed in the original paper (Larsen et al., 2006).

A PROXIMAL TUBULE MODEL

Data from mammalian (rat, rabbit) proximal convoluted tubule were used to model epithelial cells and interspace with luminal and peritubular baths of identical composition, $C_{Na^+}^{lumen} = C_{Na^+}^{serosa} = 145$ mM, $C_{K^+}^{lumen} = C_{K^+}^{serosa} = 5$ mM, $C_{Cl^-}^{lumen} = C_{Cl^-}^{serosa} = 150$ mM, resulting in quantities listed in Table 3 together with corresponding experimental data. Both intracellular concentrations and the membrane conductances are simulated reasonably well. The transepithelial osmotic permeability of the reference model epithelium is $P_f = 0.31$ cm·s⁻¹ with a reversal of water flow for $\Delta\pi_{rev} = -11$ mOsm (lumen hyperosmotic). The corresponding numbers for mammalian proximal tubule are $P_f = 0.24$ – 0.35 cm·s⁻¹ (Schafer & Andreoli, 1979; Weinstein, 1992) and $\Delta\pi_{rev} = -11$ or -20 mOsm, depending on the peritubular protein concentration (Green et al., 1991). The associated transepithelial fluxes are (pmol·cm⁻²·s⁻¹) $J_{Na} = 9277$, $J_K = 321$, $J_{Cl} = 9598$ and with a transepithelial volume flow of 62.1 nL·cm⁻²·s⁻¹ the computed composition of the absorbate is $C_{Na^+}^{abs} = 149.4$ mM, $C_{K^+}^{abs} = 5.2$ mM, and $C_{Cl^-}^{abs} = 154.6$ mM, that is, the nominal osmotic

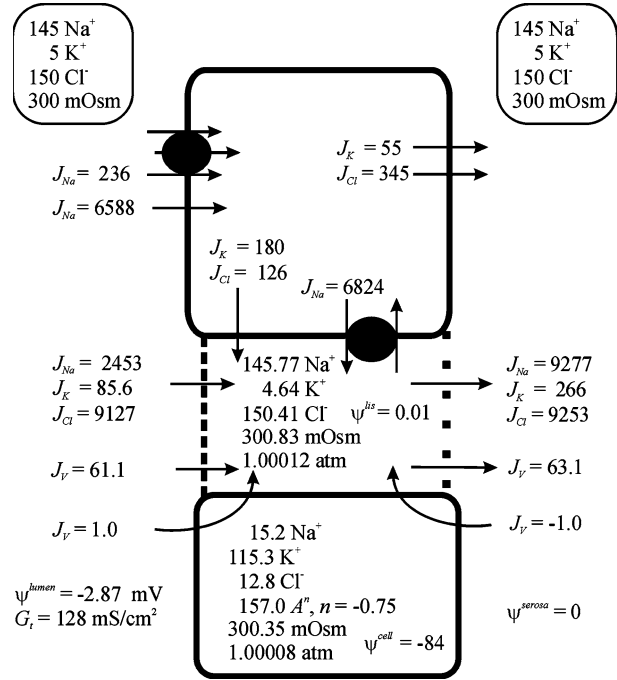


Fig. 6. Reference state of mammalian kidney proximal tubule model with Na⁺ recirculation turned off. Luminal and serosal baths of similar composition: $C_{Na^+}^{lumen} = C_{Na^+}^{serosa} = 145$ mM, $C_{K^+}^{lumen} = C_{K^+}^{serosa} = 5$ mM, and $C_{Cl^-}^{lumen} = C_{Cl^-}^{serosa} = 150$ mM. Computed ion concentrations are in mM, electrical potentials in mV, ion fluxes in pmol·cm⁻²·s⁻¹, and volume flow is in nl·cm⁻²·s⁻¹. The high hydraulic permeability of apical barriers results in concentrations of ions in the lateral space very close to those of baths. The sodium concentration of the emerging fluid is $J_{Na}^{lumen}/J_V^{lumen} = 9277/63.1 = 147.0$ mM and if truly isosmotic transport is demanded, the associated recirculation flux would be 4.1% (see Fig. 7D).

concentration of the transported fluid is 309 mOsm. Thus, accounting for the major fluxes and hydrosmotic and bioelectrical features integrated in an overall satisfying description of the tubular epithelium, the reference model produces a 3% hyperosmotic absorbate. In an experimental nephron preparation, most likely, this would be judged isosmotic within experimental errors.

NEAR-ISOSMOTIC AND TRULY ISOSMOTIC TRANSPORT

Fig. 6. depicts the model epithelium with intraepithelial concentrations together with the associated water and ion fluxes. It is noted that this model

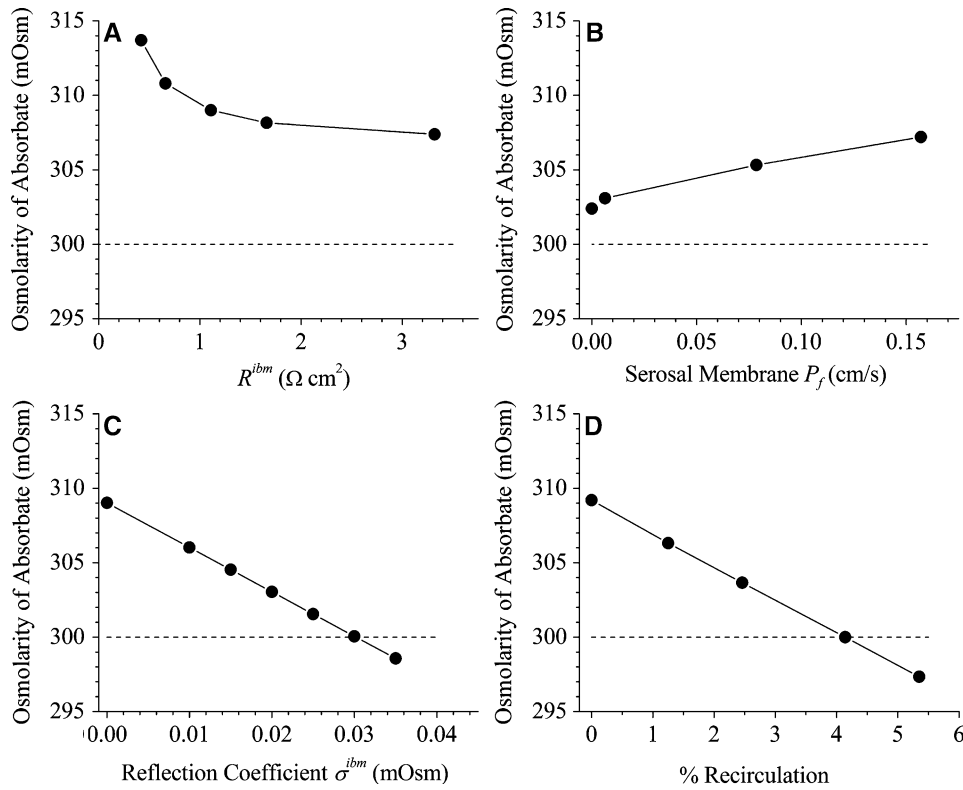


Fig. 7. In the highly water-permeable proximal tubule isosmotic transport is achieved by metabolically neutral mechanisms and mechanisms requiring investment of metabolic energy. *A.* Computations predict raised osmolarity of the absorbate with increasing ion permeability of the interspace basement membrane (*conf.* Fig. 2). *B.* Eliminating exit fluxes through the serosal plasma membrane and reducing the osmotic permeability of this membrane leads to an osmolarity of the absorbate that is isosmotic within 1%. *C.* As expected (text Eq. 2), a small reflection coefficient of *ibm*, here $\sigma = 0.03$, results in isosmotic transport. *D.* Ion recirculation constitutes a fourth mechanism by which isosmotic transport is achieved (Larsen et al., 2006).

simulating major bioelectric and hydrosmotic features well (*see* also Table 3) predicts the fluid in the lateral space of mammalian proximal tubule to be isosmotic within less than 1 mOsm with $C_{\text{Na}^+}^{\text{lis}} = 145.8$ mM. Nevertheless, the sodium concentration of the fluid emerging from the lateral space is $9277/63.1 = 147.0$ mM. This is obtained with a resistance of the interspace basement membrane of $R^{ibm} = 1.1 \Omega \cdot \text{cm}^2$. With a tight junction resistance of $7.0 \Omega \cdot \text{cm}^2$, this value of R^{ibm} may be in the upper range of possible physiological values. Varying this parameter between 0.4 and $3.3 \Omega \cdot \text{cm}^2$ resulted in a computed range of osmolarities of the absorbate between 314 and 307 mOsm while the osmotic concentration of the interspace fluid changed by less than 0.02 mOsm about a value of 300.85 mOsm (Fig. 7A). This result underscores the decisive influence of the permeability of the interspace basement membrane on the osmotic concentration of the absorbate. The computations also indicate that within the range of likely permeabilities of the interspace basement membrane the osmotic concentration of the absorbate varies from values that are so close to the osmotic concentration of the surrounding solutions that the difference cannot possibly be detected to values that would impose a significant extracellular salt load on the organism. It would be expected (Eq. 2) that the absorbate's osmolarity approaches that of the *lis* (and bath) if R^{ibm} becomes sufficiently large (Fig. 2). Nevertheless, the computed osmolarity approaches a value of about 306 mOsm for large R^{ibm} (Fig. 7A). This is a trivial consequence of

solute fluxes directed from cells into the serosal bath and of water uptake across the serosal plasma membrane (Fig. 6). If the exit of ions from the cells is entirely via the lateral plasma membrane and the recirculation of water across inner barriers is suppressed by reducing the serosal membrane's osmotic permeability the absorbate's osmolarity approaches the tonicity of the bathing solution within less than 1% (Fig. 7B). With all fluxes of the serosal membrane eliminated, computations predicted $P_f = 0.12$ cm/s with a reversal of water flow for $\Delta\pi_{\text{rev}} = -29$ mOsm (*not shown* in figures). In principle and for all practical purposes this might be a mechanism for achieving isosmotic transport. It should be noted, however, that immunoperoxidase labeling has localized AQP1 to all three plasma membrane domains of proximal tubule (Nielsen et al., 2002), which makes this way of obtaining isosmotic transport unlikely. Following Sackin & Boulpaep (1975), another way of reducing the tonicity of the absorbate would be to introduce a finite reflection coefficient of the interspace basement membrane as depicted in Fig. 7C. In the example shown, with $\sigma^{ibm} = 0.03$ of all three diffusible ions, the concentrations of the absorbate are $C_{\text{Na}^+}^{\text{abs}} = 145.0$ mM, $C_{\text{K}^+}^{\text{abs}} = 5.0$ mM, and $C_{\text{Cl}^-}^{\text{abs}} = 150.0$ mM. The quantitative morphometric analysis by Welling et al. (1987) indicated that the basal region of the tubular space may constitute a resistive barrier for fluxes out of *lis*. It is unknown whether this is compatible with a finite, however small, reflection coefficient for small ions. A fourth

Table 4. Hydraulic (L_P) and osmotic water (P_f) permeabilities of the kidney model. L_P is expressed in SI units used in the Fortran program and in three frequently used units in physiological literature.

Unit	(m/s)/(N/m ²)	L_P cm ³ /(cm ² ·s) per osm/kg	cm ³ /(cm ² ·s) per mmHg	cm ³ /(cm ² ·s) per atm	P_f cm/s
Apical plasma membrane	$1.10 \cdot 10^{-11}$	$2.83 \cdot 10^{-3}$	$1.47 \cdot 10^{-7}$	$1.11 \cdot 10^{-4}$	0.157
Basal plasma membrane	$1.10 \cdot 10^{-11}$	$2.83 \cdot 10^{-3}$	$1.47 \cdot 10^{-7}$	$1.11 \cdot 10^{-4}$	0.157
Lateral plasma membrane	$1.60 \cdot 10^{-11}$	$4.12 \cdot 10^{-3}$	$2.13 \cdot 10^{-7}$	$1.62 \cdot 10^{-4}$	0.229
Tight junction*	$5.00 \cdot 10^{-10}$	$1.29 \cdot 10^{-1}$	$6.67 \cdot 10^{-6}$	$5.07 \cdot 10^{-3}$	7.16
Interspace basement membrane	$5.00 \cdot 10^{-8}$	$1.29 \cdot 10^1$	$6.67 \cdot 10^{-4}$	$5.07 \cdot 10^{-1}$	716

*It should be noted that there is a significant difference between computed transepithelial osmotic permeability of the AQP(-/-) simulation, $P_f = 0.078$ cm·s⁻¹ (Fig. 8) and the tight junction's osmotic permeability, $P_f^{ij} = 7.16$ cm·s⁻¹, listed in Table 4. This discrepancy follows logically from the osmotic effect of the external non-permeant solute being opposed by the osmotic effect of accumulated ions in *lis*, which means that the true driving force for water uptake becomes small ('intraepithelial solute polarization', Weinstein & Stephenson 1981).

putational results, we obtained a shunt conductance of $7.8 \Omega \cdot \text{cm}^2$, a transepithelial potential difference of -4.4 mV, $C_{\text{Na}^+}^{\text{lis}} = 145.5$ mM, $C_{\text{K}^+}^{\text{lis}} = 4.66$ mM, $C_{\text{Cl}^-}^{\text{lis}} = 150.2$ mM, $J_v = 43.1$ nl cm⁻²·s⁻¹, and an osmolality of the absorbate of 308 mOsm. However, computations also predicted that the reabsorbed Na⁺ flux being less than the pumped Na⁺-flux, *in casu*, $J_{\text{Na}^+}^{\text{transepit}}/J_{\text{Na}^+}^{\text{pump}} = 0.95$ associated with a continuous loss of Na⁺ from *lis* into the luminal bath through tight junctions, $J_{\text{Na}^+}^{\text{ij}} = -308$ pmol·cm⁻²·s⁻¹. This result is in accordance with computations obtained with the 'electroneutral' model, *see* Larsen et al. (2000), which contains a more detailed discussion of the issue, and it predicts previous experimental studies on MDCK cells in which tight junctions were shown to be Na⁺-permeable (Kovbasnjuk et al., 1995) but water-tight (Kovbasnjuk et al., 1998). Therefore, model simulation of pseudo-solvent drag together with the above experimental observations on intact mammalian kidney showing reabsorption of Na⁺ with high metabolic efficiency ($\text{Na}^+/\text{O}_2 = 28\text{--}32$) add further evidence that paracellular solute uptake under equilibrium conditions cannot be driven by pseudo-solvent drag.

Mammalian kidney proximal tubule is just one example of leaky epithelia with high metabolic efficiency of Na⁺ absorption. In a study of rabbit gallbladder Martin & Diamond (1966) showed that the ratio of the sodium flux near transepithelial equilibrium and the associated oxygen uptake is about 24 Na⁺/O₂. In a subsequent study Frederiksen and Leyssac, 1969, confirmed the high metabolic efficiency in rabbit gallbladder by reporting 30 Na⁺/O₂ and they showed that the ratio dropped to about 13 Na⁺/O₂ upon dilution of the bathing solutions to half Ringer's strength. In a previous model study gallbladder data were simulated that predicted a significant drop of the Na⁺/O₂ ratio, from 25 to 12 Na⁺/O₂, as a result of diluting the external compartments from 300 to 50 mOsm with no other changes of independent variables (Larsen et al., 2000). Like the kidney

example above, in gallbladder the Na⁺/O₂ ratio > 18 is the result of the recirculation flux being smaller than the paracellular convective uptake of Na⁺. Upon dilution of the luminal bath the computations predicted that the paracellular convection flux of Na⁺ is being reduced relatively much more than the recirculation flux, thus providing a logical explanation for the experimental findings. In experiments with the biological preparations the rate of fluid uptake was significantly stimulated by diluting the external baths. This result was not predicted in our model simulations. To reproduce this finding as well, the apical entrance mechanism for Na⁺ would have to be stimulated independently of bath dilutions.

In summary, the treatment above with water-permeable tight junctions fulfills the requirement of predicting solvent drag. The evidence for water-permeable tight junctions is indirect, but taken together our discussions above lead us to the conclusion that a significant number of experimental observations find their logical explanation if it is assumed that tight junctions are water permeable. Thus, our analysis has indicated significant physiological functions of tight junctions by reconciling the surprisingly low metabolic cost of Na⁺ reabsorption and the low electrical resistance of the paracellular pathway. Further consequences of a finite water permeability of tight junctions are discussed below.

WATER FLUXES AND HYDRAULIC PERMEABILITIES

Table 4 lists the standard model's hydraulic permeabilities (Larsen et al., 2006). L_P and its equivalent osmotic permeability, P_f , is listed in the frequently used units and in SI units (used in our computer program). Below, these numbers will be discussed together with the osmotic water permeability of the epithelium obtained by the conventional protocol in which a non-permeating electroneutral molecule at different concentrations is added to the bathing solutions while the transepithelial volume flow is recorded. With this protocol, according to computed

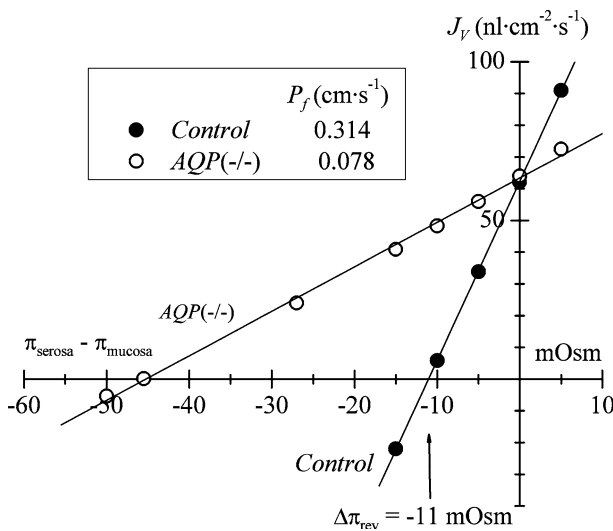


Fig. 8. Imposing a difference of osmotic concentration across the model epithelium reveals capacity for uphill water transport with reversal of water flow for $\Delta\pi = -11$ mOsm (luminal bath hyperosmotic) and a tissue osmotic permeability of $0.314 \text{ cm}\cdot\text{s}^{-1}$. Elimination of the hydraulic permeability of all three plasma membranes (*am*, *sm*, and *lm*) for simulating the AQP1 knockout mouse predicts a residual osmotic permeability of $0.078 \text{ cm}\cdot\text{s}^{-1}$. The rate of water absorption for $\Delta\pi = 0$ is practically unaffected. Modified from Larsen et al. (2006).

results, the model is exhibiting uphill water transport with an osmotic permeability, $P_f = 0.31 \text{ cm}\cdot\text{s}^{-1}$ and reversal of water flow for $\Delta\pi_{\text{rev}} = -11$ mOsm ('control' of Fig. 8). As mentioned above, these numbers are in reasonable agreement with measured values of mammalian proximal tubule. Eliminating the hydraulic permeability of all three plasma membranes for simulating the aquaporin-1 knockout mouse reduced P_f by 75% [AQP(-/-), Fig. 8]², which should be compared to a reduction of 78% in knockout mice (Schnermann et al., 1998). In the model the residual volume flow is confined to tight junctions and is driven by a hyperosmotic and hyperbaric lateral intercellular space. The y-axis intercepts are about the same for 'wild type' and 'knockout' simulations (Fig. 8). In contrast, in AQP1 knockout mice the fluid reabsorption at transepithelial osmotic equilibrium is reduced to half of the fluid reabsorption in wild-type mice (Schnermann et al., 1998), indicating a reduced active flux of Na^+ into *lis* presumably caused by down-regulation of the Na^+ flux across the apical membrane. The above analysis leads to the conclusion that the reduced volume reabsorption at osmotic

²In the AQP1(-/-) computations the relationship between J_v and $\Delta\pi$ is not strictly linear but upward concave. In the original paper P_f was estimated near equilibrium, which resulted in a somewhat larger P_f (Larsen et al., 2006).

equilibrium in knockout mice cannot be a simple direct effect of lack of expression of AQP1.

Concluding Remarks

The sodium recirculation theory for solute-coupled fluid absorption developed from experimental studies on small intestine handles truly isosmotic transport between body compartments. It is an expansion of the local osmosis concept introduced by Curran, 1960. Diamond and Bossert, 1967, analyzed physical and geometrical conditions for obtaining isosmotic transport in such a system. The sodium recirculation theory differs from that of Diamond and Bossert in assuming uniformly distributed Na^+/K^+ -pumps on the lateral membranes and ascribing a dual role of the pumps in transporting fluid from one side of the epithelium to the other. Firstly, by generating a hyperosmotic and hyperbaric lateral space the pumps provide the condition for fluid uptake at equilibrium conditions as well as against an adverse transepithelial osmotic gradient. Secondly, energy is expended also in regulating the tonicity of the transported fluid by pumping sodium ions, returning through the basal plasma membrane via Na^+ -gradient-driven transporters, back into the lateral space. Mathematical modeling of the leaky epithelium predicts such different observations as truly isosmotic transport, hyposmotic transport, solvent drag, the range of metabolic expenses associated with transepithelial Na^+ absorption, the residual hydraulic permeability in proximal tubule of AQP1(-/-) mice, and the inverse relationship between hydraulic permeability and the concentration difference needed to reverse transepithelial water flow. Thus, the mathematical model is in agreement with a wide range of experiments.

The study is supported by a frame grant from the Danish Natural Science Research Council, 272-05-0417.26

References

- Agre, P., Nielsen, S. 1996. The aquaporin family of water channels in kidney. *Néphrologie* **17**:409–415
- Barry, R.J.C., Smyth, D.H., Wright, E.M. 1965. Short-circuit current and solute transfer by rat jejunum. *J. Physiol.* **181**:410–431
- Barry, P.H., Diamond, J.M. 1984. Effects of unstirred layers on membrane phenomena. *Physiol. Rev.* **64**:763–872
- Berry, C.A. 1983. Water permeability and pathways in proximal tubules. *Am. J. Physiol.* **245**:F279–F294
- Boulpaep, E.L., Maunsbach, A.B., Tripathi, S., Weber, M.R. 1993. Mechanism of isosmotic water transport in leaky epithelia: Consensus and inconsistencies. In: Ussing, H.H., Fischbarg, J., Sten-Knudsen, O., Larsen, E.H., Willumsen, N.J., (eds) *Proc. Alfred Benzon Symp. 34, Isotonic Transport in Leaky Epithelia*. pp 53–67, Munksgaard, Copenhagen

- Cassola, A.C., Mollehauser, M., Frömter, E. 1983. The intracellular chloride activity of rat kidney proximal tubule cells. *Pflügers Arch.* **399**:259–265
- Curran, P.F. 1960. Na, Cl, and water transport by rat ileum *in vitro*. *J. Gen. Physiol.* **43**:1137–1148
- Curran, P.F., Macintosh, J.R. 1962. A model system for biological water transport. *Nature* **193**:347–348
- Curran, P.F., Solomon, A.K. 1957. Ion and water fluxes in the ileum of rats. *J. Gen. Physiol.* **41**:143–168
- Deetjen, P., Kramer, K. 1961. Die Abhängigkeit des O₂-Verbrauchs der Niere von der Na-Rückresorption. *Pflügers Arch.* **273**:636–642
- Denker, B.M., Smith, B.L., Kuhajda, P.P., Agre, P. 1988. Identification, purification, and partial characterization of a novel Mr 28000 integral membrane protein from erythrocytes and renal tubules. *J. Biol. Chem.* **263**:15634–15642
- Diamond, J.M. 1962. The reabsorptive function of the gall-bladder. *J. Physiol.* **161**:442–473
- Diamond, J.M. 1964a. Transport of salt and water in rabbit and guinea pig gall bladder. *J. Gen. Physiol.* **48**:1–14
- Diamond, J.M. 1964b. The mechanism of isotonic water transport. *J. Gen. Physiol.* **48**:15–42
- Diamond, J.M., Bossert, W.H. 1967. Standing gradient osmotic flow. A mechanism for coupling of water and solute transport in epithelia. *J. Gen. Physiol.* **50**:2061–2083
- Edelman, A., Curci, S., Samarzija, I., Frömter, E. 1978. Determination of intracellular K⁺ activity in rat kidney proximal tubular cells. *Pflügers Arch.* **378**:37–45
- Finkelstein, A. 1987. Water movement through lipid bilayers, pores, and plasma membranes. Theory and Reality. John Wiley & Sons, New York,
- Fischbarg, J., Diecke, F.P.J. 2005. A mathematical model of electrolyte and fluid transport across corneal epithelium. *J. Membrane Biol.* **203**:41–56
- Frederiksen, O., Leyssac, P.P. 1969. Transcellular transport of isosmotic volumes by rabbit gall-bladder *in vitro*. *J. Physiol.* **201**:201–224
- Frizzell, R.A., Schultz, S.G. 1972. Ionic conductances of extracellular shunt pathway in rabbit ileum. Influence of shunt on transmural sodium transport and electrical potential differences. *J. Gen. Physiol.* **59**:318–346
- Frömter, E. 1979. Solute transport across epithelia: what can we learn from micropuncture studies on kidney tubules? *J. Physiol.* **288**:1–31
- Frömter, E., Rumrich, G., Ullrich, K.J. 1973. Phenomenologic description of Na⁺, Cl⁻ and HCO₃⁻ absorption. *Pflügers Arch.* **343**:189–220
- Green, R., Giebisch, G. 1984. Luminal hypotonicity: a driving force for fluid absorption from the proximal tubule. *Am. J. Physiol.* **246**:F167–F117
- Green, R., Giebisch, G., Unwin, R., Weinstein, A.M. 1991. Coupled water transport by rat proximal tubule. *Am. J. Physiol.* **261**:F1046–F1054
- Gögelein, H., Greger, R. 1986. Na⁺ selective channels in the apical membrane of rabbit late proximal tubule (pars recta). *Pflügers Arch.* **406**:198–203
- Guggino, W.B., London, R., Boulpaep, E.L., Giebisch, G. 1983. Chloride transport across the basolateral cell membrane of the *Necturus* proximal tubule. *J. Membrane Biol.* **71**:227–240
- Halm, D.R., Krasny, E.J., Frizzell, R.A. 1985a. Electrophysiology of flounder intestinal mucosa. I. Conductance properties of the cellular and paracellular pathways. *J. Gen. Physiol.* **85**:843–864
- Halm, D.R., Krasny, E.J., Frizzell, R.A. 1985b. Electrophysiology of flounder intestinal mucosa. II. Relation of the electric potential to coupled Na-Cl absorption. *J. Gen. Physiol.* **85**:865–883
- Hertz, G. 1922. Ein neues Verfahren zur Trennung von Gasgemischen durch Diffusion. *Physik. Z.* **23**:433–434
- Jørgensen, P.L. 1980. Sodium and potassium ion pump in kidney tubules. *Physiol. Rev.* **60**:864–917
- Karniski, L.P., Aronson, P.S. 1985. Chloride/formate exchange with formic acid recycling: A mechanism of active chloride transport across epithelial membranes. *Proc. Natl. Acad. Sci. USA* **82**:6362–6365
- Kashgarian, M., Biemesderfer, C., Caplan, M., Forbush, B. 1985. Monoclonal antibody to Na,K-ATPase: immunocytochemical localization along nephron segments. *Kidney Intern.* **28**:899–913
- Kovbasnjuk, O., Chatton, J.-Y., Friauf, W.S., Spring, K.R. 1995. Determination of the sodium permeability of the tight junctions of MDCK cells by fluorescence microscopy. *J. Membrane Biol.* **148**:223–232
- Kovbasnjuk, O., Leader, J.P., Weinstein, A.M., Spring, K.R. 1998. Water does not flow across the tight junctions of MDCK cell epithelium. *Proc. Natl. Acad. Sci. USA* **95**:6526–6530
- Larsen, E.H., Sørensen, J.B., Sørensen, J.N. 2000. A mathematical model of solute coupled water transport in toad small intestine incorporating recirculation of the actively transported solute. *J. Gen. Physiol.* **116**:101–124
- Larsen, E.H., Sørensen, J.B., Sørensen, J.N. 2002. Topical Review: Analysis of the sodium recirculation theory of solute-coupled water transport in small intestine. *J. Physiol.* **542**:33–50
- Larsen, E.H., Møbjerg, N., Sørensen, J.N. 2006. Fluid transport and ion fluxes in mammalian kidney proximal tubule: A model analysis of isotonic transport. *Acta Physiol.* **187**:177–189
- Lassen, U.V., Thaysen, J.H. 1961. Correlation between sodium transport and oxygen consumption in isolated renal tissue. *Biochim. Biophys. Acta* **47**:616–618
- Lassen, N.A., Munk, O., Thaysen, J.H. 1961. Oxygen consumption and sodium reabsorption in the kidney. *Acta Physiol. Scand.* **51**:371–384
- Loo, D.D.F., Zeuthen, T., Chandy, G., Wright, E.M. 1996. Cotransport of water by the Na⁺/glucose cotransporter. *Proc. Natl. Acad. Sci. USA* **93**:13367–13370
- Martin, D.W., Diamond, J.M., 1996. Energetics of coupled active transport of sodium and chloride. *J. Gen. Physiol.* **50**:295–315
- Mathias, R.T., Wang, H. 2005. Local osmosis and isotonic transport. *J. Membrane Biol.* **208**:39–53
- Meinild, A.-K., Klærke, D.A., Loo, D.D.F., Wright, E.M., Zeuthen, T. 1998. The human Na⁺/glucose transporter is a molecular water pump. *J. Physiol.* **508**:15–21
- Morel, F., Murayama, Y. 1970. Simultaneous measurement of unidirectional and net sodium fluxes in microperfused rat proximal tubules. *Pflügers Arch.* **320**:1–23
- Naftalin, R.J., Tripathi, S. 1986. The roles of paracellular and transcellular pathways and submucosal space in isotonic water absorption by rabbit ileum. *J. Physiol.* **370**:409–432
- Nedergaard, S., Larsen, E.H., Ussing, H.H. 1999. Sodium recirculation and isotonic transport in toad small intestine. *J. Membrane Biol.* **168**:241–251
- Nielsen, S., Frøkiær, J., Marples, D., Kwon, T.-H., Agre, P., Knepper, M. 2002. Aquaporins in the kidney: From molecules to medicine. *Physiol. Rev.* **82**:205–244
- Parsons, D.S., Wingate, D.L. 1958. Fluid movements across the wall of rat small intestine. *Biochim. Biophys. Acta.* **30**:666–667
- Preston, G.M., Caroll, T.P., Guggino, W.B., Agre, P. 1992. Appearance of water channels in *Xenopus* oocytes expressing red cell CHIP28 protein. *Science* **257**:385–387
- Pihakaski-Maunsbach, K., Vorum, E.L., Locke, E.-M., Garty, H., Karlish, S.J.D., Maunsbach, A.B. 2003. Immunocytochemical localization of Na,K-ATPase gamma subunit and CHIP in inner medulla of rat kidney. *Ann. N. Y. Acad. Sci.* **986**:401–409

- Rector, F.C. 1983. Sodium, bicarbonate and chloride absorption by proximal tubule. *Am. J. Physiol.* **244**:F461–F471
- Rubashkin, A., Iserovich, P., Hernandez, J.A., Fischbarg, J. 2005. Epithelial transport: protruding macromolecules and space charges can bring about electro-osmosis at the tight junctions. *J. Membrane Biol.* **208**:251–263
- Sackin, H., Boulpaep, E.L. 1975. Models for coupling of salt and water transport. Proximal tubular reabsorption in *Necturus* kidney. *J. Gen. Physiol.* **66**:671–733
- Sanchez, J.M., Rubashkin, A., Iserovich, P., Wen, Q., Ruberti, J.W., Smith, R.W., Rittenband, D., Kuang, K., Diecjkje, F.P.J., Fischbarg, J. 2002. Evidence for a central role for electro-osmosis in fluid transport by comeal endothelium. *J. Membrane Biol.* **187**:37–50
- Schafer, J.A. 1990. Transepithelial osmolality differences, hydraulic conductivities, and volume absorption in the proximal tubule. *Annu. Rev. Physiol.* **52**:709–726
- Schafer, J.A., Andreoli, T.E. 1979. Perfusion of isolated mammalian renal tubules. In: Giebisch, G., (ed) *Transport Biology Volume 4: Transport Organs*. pp 473–528, Springer-Verlag, Berlin
- Schafer, J.A., Patlak, C.S., Andreoli, T.E. 1975. A component of fluid absorption linked to passive ion flows in the superficial pars recta. *J. Gen. Physiol.* **66**:445–471
- Schermann, J., Chou, J., Ma, T., Traynor, T., Knepper, M.A., Verkman, A.S. 1998. Defective proximal fluid reabsorption in transgenic aquaporin-1 null mice. *Proc. Natl. Acad. Sci. USA* **95**:9660–9664
- Schultz, S.G. 2001. Epithelial water absorption: Osmosis or Co-transport? *Proc. Natl. Acad. Sci. USA* **98**:3628–3630
- Smyth, D.H., Wright, E.M. 1966. Streaming potentials in the rat small intestine. *J. Physiol.* **182**:591–602
- Spring, K.R. 1998. Routes and mechanisms of fluid transport by epithelia. *Ann. Rev. Physiol.* **60**:105–119
- Spring, K.R., Hope, A. 1979. Fluid transport and the dimensions of cells and interspaces of living *Necturus* gallbladder. *J. Gen. Physiol.* **73**:287–305
- Sten-Knudsen, O. 2002. Biological membranes. Theory of transport, potentials and electric impulses. Cambridge University Press, Cambridge
- Sten-Knudsen, O., Ussing, H.H. 1981. The flux ratio equation under nonstationary conditions. *J. Membrane Biol.* **63**:233–242
- Stirling, C.E. 1972. Radioautographic localization of sodium pump sites in rabbit intestine. *J. Cell. Biol.* **53**:704–714
- Thurau, K. 1961. Renal reabsorption and O₂ uptake in dogs during hypoxia and hydrochloro-thiazide infusion. *Proc. Soc. Exp. Biol. Med.* **106**:714–717
- Tripathi, S., Boulpaep, E.L. 1989. Mechanisms of water transport by epithelial cells. *Quart. J. Exp. Physiol.* **74**:385–417
- Torrelli, G.E., Milla, E., Faelli, A., Costantini, S. 1966. Energy requirement for sodium reabsorption in the in vivo rabbit kidney. *Am. J. Physiol.* **211**:576–580
- Ullrich, K. 1973. Permeability characteristics of the mammalian nephron. In: Orloff, J., Berliner, B.W., (eds) *Handbook of Physiology. Section 8: Renal Physiology*. pp 377–398, American Physiological Society, Bethesda
- Ussing, H.H. 1949. The distinction by means of tracers between active transport and diffusion. *Acta Physiol. Scand.* **19**:43–56
- Ussing, H.H., Eskesen, K. 1989. Mechanism of isotonic water transport in glands. *Acta Physiol. Scand.* **136**:443–454
- Ussing, H.H., Lind, F., Larsen, E.H. 1996. Ion secretion and isotonic transport in frog skin glands. *J. Membrane Biol.* **152**:101–110
- Ussing, H.H., Nedergaard, S. 1993. Recycling of electrolytes in small intestine of toad. In: Ussing, H.H., Fischbarg, J., Sten-Knudsen, O., Larsen, E.H., Willumsen, N.J., (eds) *Proc. Alfred Benzon Symp. 34, Isotonic Transport in Leaky Epithelia*. pp 25–34, Munksgaard, Copenhagen
- Vallon, V., Verkman, A.S., Schnermann, J. 2000. Luminal hypotonicity in proximal tubule of aquaporin-1-knockout mice. *Am. J. Physiol.* **278**:F1030–F1033
- Welling, L.W., Welling, D.J., Holsapple, J.W., Evan, A.P. 1987. Morphometric analysis of distinct microanatomy near the base of proximal tubule cells. *Am. J. Physiol.* **253**:F126–F140
- Weinstein, A.M. 1986. A mathematical model of the rat proximal tubule. *Am. J. Physiol.* **250**:F860–F873
- Weinstein, A.M. 1992. Sodium and chloride transport. In: Seldin, D.W., Giebisch, G., (eds) *The Kidney Physiology and Pathophysiology, 2nd edition* Vol 2: pp 1925–1973, Raven Press, New York
- Weinstein, A.M. 1994. Mathematical models of tubular transport. *Annu. Rev. Physiol.* **56**:691–709
- Weinstein, A.M. 2003. Mathematical models of renal fluid and electrolyte transport: acknowledging our uncertainty. *Am. J. Physiol.* **284**:F871–F884
- Weinstein, A.M., Stephenson, J.L. 1981. Models of coupled salt and water transport across leaky epithelia. *J. Membrane Biol.* **60**:1–20
- Whitlock, R.T., Wheeler, H.O. 1964. Coupled transport of solute and water across rabbit gallbladder epithelium. *J. Clin. Invest.* **43**:2249–2265
- Whittembury, G., Paz-Aliaga, A., Biondi, A., Carpi-Medina, P., Gonzales, E., Linares, H. 1985. Pathways for volume flow and volume regulation in leaky epithelia. *Pflügers Arch. Eur. J. Physiol.* **404**:S17–S22
- Whittembury, G., Malnic, G., Mello-Aires, M., Amorena, C. 1988. Solvent drag of sucrose during absorption indicates paracellular water flow in the rat kidney proximal tubule. *Pflügers Arch. Eur. J. Physiol.* **412**:541–547
- Whittembury, G., Reuss, L. 1992. Mechanism of coupling of solute and solvent transport in epithelia. In: Seldin, D.W., Giebisch, G., (eds) *The Kidney Physiology and Pathophysiology, 2nd edition* Vol 1. pp 317–360, Raven Press, New York
- Whittembury, G., Echevania, M., Gutierrez, A., Gonzales, E. 1993. Absorption of salt and water in the proximal tubule. In: Ussing, H.H., Fischbarg, J., Sten-Knudsen, O., Larsen, E.H., Willumsen, N.J., (eds) *Proc. Alfred Benzon Symp. 34, Isotonic Transport in Leaky Epithelia*. pp 37–48, Munksgaard, Copenhagen
- Windhager, E.E. 1979. Sodium chloride transport. In: Giebisch, G., (ed) *Membrane Transport in Biology Volume IV. Transport Organs*. pp 145–214, Springer-Verlag, Berlin
- Windhager, E.E., Whittembury, G., Oken, D.E., Schatzmann, H.J., Solomon, A.K. 1958. Single proximal tubules of the *Necturus* kidney. III. Dependence of H₂O movement on NaCl concentration. *Am. J. Physiol.* **197**:313–318
- Yoshitomi, K., Frömter, E. 1985. How big is the electrochemical potential difference of Na⁺ across rat renal proximal tubular cell membranes *in vivo*? *Pflügers Arch.* **405**:S121–S126
- Zeuthen, T., Belhage, B., Zeuthen, E. 2006. Water transport by Na⁺-coupled cotransporters of glucose (SGLT1) and of iodide (NIS). The dependence of substrate size at high resolution. *J. Physiol.* **570**:485–499